Coherent linear optical sampling at 15 bits of resolution

I. Coddington,* W. C. Swann, and N. R. Newbury

National Institute of Standards and Technology, 325 Broadway, Boulder, Colorado 80305, USA
Corresponding author: ian@nist.gov

Linear optical sampling characterizes a sample by measuring the distortions on a transmitted optical field, thereby quantifying the sample's optical response. By exploiting the high mutual coherence between two phase-locked femtosecond fiber lasers, we achieve very high signal-to-noise ratio measurements of transmitted optical electric fields through coherent averaging. We measure the optical electric fields with 15.16 bits of dynamic range (91 dB in intensity) and with 525 fs timing resolution over a 10 ns time window, in a 5.1 s averaging period.
    OCIS codes: 320.7100, 140.4050, 120.3180.

High-resolution measurements of optical response are useful in a wide range of applications that include telecommunications and ultrafast science for component characterization, spectroscopy, or laser radar. The optical response can be measured by comparing the electric field of a test pulse before and after the sample [1–5]. In linear optical sampling (LOS), the test pulses are heterodyned against a reference pulse with a varying time delay, thereby effectively measuring their electric-field cross correlation [1]. LOS has the particular advantage of compatibility with recent advances in coherent frequency combs [6–9]. Here, we discuss implementation of LOS with two mutually coherent frequency combs to realize coherent linear optical sampling (CLOS). CLOS is the time-domain equivalence of multiheterodyne comb spectroscopy [10–15] and is analogous to time-domain terahertz spectroscopy [16]. In recent work, we exploited the high bandwidth and the speed of CLOS for precision ranging [17], and we exploited the high frequency resolution of its frequency-domain counterpart, multiheterodyne spectroscopy, for precision molecular spectroscopy [13]. In this Letter we focus on the ability of CLOS to leverage the mutual coherence of tightly phase-locked combs into high signal-to-noise ratio (SNR) time-domain measurements of optical electric fields while maintaining the frequency accuracy and the resolution specific to comb-based measurements.

Standard techniques for stabilizing frequency combs (i.e., femtosecond lasers) produce a precise ruler for frequency metrology [6,7]; in the time domain, they also yield a low jitter highly coherent pulse train [8,9]—an ideal source for CLOS. The basic concept of CLOS remains the same as LOS; the pulses from a "signal" comb are transmitted through the test sample while the pulses from a second "local oscillator" (LO) comb interrogate the distorted signal pulses to measure the optical response (see Fig. 1). The high mutual optical coherence of the signal and the LO combs in conjunction with a well-controlled difference in their pulse repetition rates enables repeated measurements of the distorted signal field, providing a fine time resolution and a high SNR. We achieve nearly shot-noise-limited detection with av-eraging periods limited only by the source coherence time (or in our case by digitizer memory).

As a simple demonstration, the signal comb pulse is split to generate a reference pulse before, and a test pulse after, transmission through a ~1 km fiber spool (see Fig. 1). The two pulses are then combined with a ~3 ns separation (much longer than the pulse duration) and the LO pulse samples the electric fields with 525 fs time steps and femtosecond level jitter over a 10 ns time window. With a 5.1 s averaging period, we achieve a SNR of 36,700, corresponding to 15.16 bits of dynamic range (91 dB in optical intensity). For our reference pulse energy of 8 fJ, the 91 dB dynamic range corresponds to a sensitivity equivalent to 0.000 05 signal photons (6×10^{-24} J) per 525 fs time bin for the fully averaged data.

It is interesting to compare CLOS to Fourier-transform spectral interferometry (FTSI) where the test and the reference pulses are heterodyned on a
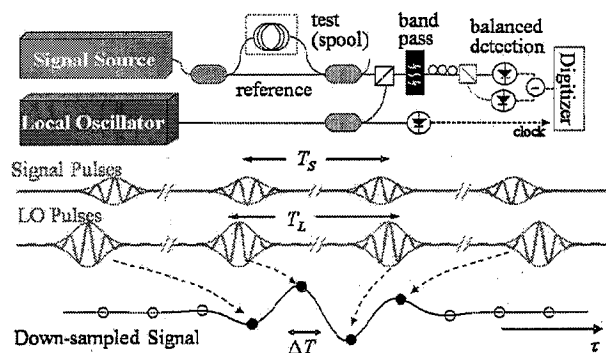

Fig. 1. (Color online) Top, schematic of the setup. The signal and the LO are two fiber frequency combs, phase locked together such that the LO pulse advances past the signal pulse by ΔT every pulse. The solid curves are fiber optics, the dashed curves are electrical paths, and the filled ovals are fiber couplers. The bandpass filter is ~2 nm wide. For the demonstration here, we used a 1.14 km spool of optical fiber as the test sample. Furthermore, we take advantage of the 10 ns time window by interleaving the "reference" and the "test" signals with a 3 ns time offset rather than detecting them separately. Balanced detection is used to achieve close to shot-noise-limited heterodyne detection. Bottom, schematic of coherent LOS assuming zero carrier-envelope offset phase for the LO pulse train.

spectrometer and the resulting spectral interference yields the relative spectral phase [2–5]. With careful spectrometer calibration [18], FTSI can provide ~10 mrad spectral phase resolution at a frequency resolution slightly worse than the underlying spectrometer, or 10–100 GHz, over a spectral width of tens of nanometers (set by the optical source bandwidth). In CLOS, the challenge of spectrometer calibration has been replaced with the challenge of operating two mutually coherent fiber combs. Here we show <1 mrad spectral (statistical) phase noise at a frequency resolution of ~300 MHz. The spectral width of a few nanometers demonstrated here could be extended to the source bandwidth (125 nm) as in [13] with no degradation of frequency resolution. In a different setup using dual interferometers [10,13,15], the individual comb teeth are resolved, improving the frequency resolution at the cost of an extra detection channel and processing.

The basic approach is illustrated in Fig. 1. The signal comb source produces a train of pulses, $E_S(t) = e^{i\varphi_S}e^{-i2\pi\nu_0 t}\Sigma_{n_S}A_S(t-n_S T_S)$, with a pulse envelope A_S, a pulse period T_S, and a phase φ_S. The LO comb has the same form, with the subscript $S \rightarrow L$. Both combs share a common tooth at optical frequency ν_0, which simplifies the treatment. The two combs are mixed, and the resulting detected heterodyne signal is $V(t) = R(t) \otimes [E_L^*(t)E_S(t)]$, where $R(t)$ is the combined response of the detector and any software filter and $\otimes$ represents a convolution. The voltage is digitized synchronously with the LO pulses. Assuming only the immediate LO pulse contributes to the voltage signal [i.e., the detector response $R(t)$ is fast relative to T_L], the digitized voltage is $V(t=n_L T_L) = \Sigma_k e^{i\Delta\varphi}\int R(t')A_L^*(-t')A_S(n_L\Delta T - t' - kT_S)dt'$, where $k = n_S - n_L$ and $\Delta T = T_L - T_S$. Switching to equivalent time $\tau = n_L\Delta T$ (see Fig. 1), the digitized voltage samples are

$$V(\tau) = e^{i\Delta\varphi}S(\tau) \otimes A_S(\tau) \otimes \sum_k \delta(\tau - kT_S) + \sigma, \quad (1)$$

where $S(\tau) \equiv R(\tau)A_L^*(-\tau)$, $\Delta\varphi = \varphi_S - \varphi_L$, and σ represents any additive noise per sample. The waveform $V(\tau)$ repeats every T_S in equivalent time and is the signal electric field sampled by $S(t)$ at a spacing of ΔT. As with any equivalent time sampling, the laboratory time scale is magnified by a factor $M = T_L/\Delta T$. The effective sampling time ΔT imposes a Nyquist limit to the maximum optical pulse bandwidth of less than $(2\Delta T)^{-1}$. To avoid aliasing of the detected signal, it is bandpassed so that $R(t)$ is, in fact, not short compared to T_L. In that case, the sampling function includes contributions from neighboring pulse pairs and is $S(\tau) = \Sigma_p R(\tau + pT_S)A_L^*(-\tau + p\Delta T)$, which for properly bandwidth-limited signals equals $S(\tau) = R(M\tau) \otimes A_L^*[-M\tau/(M-1)]$.

The sum in Eq. (1) reflects the repetitive nature of the measurement. As the LO pulse train advances across the signal pulse train, it will eventually sample a full pulse repetition period T_S (or "frame"), at which point the sampling effectively cycles around

and begins again. Acquiring a frame takes $T_S/\Delta T = M - 1$ pulses or a period $T_{update} = (M-1)T_L$ in the laboratory. Here we consider synchronous sampling defined by forcing M to be an integer. In this case, each frame has the same time offset, and one can average many frames (e.g., 26,900 here) to suppress additive Gaussian noise, σ, present from detector noise, the amplified spontaneous emission, or the shot noise. To measure the linear optical response, $H(t)$, the reference signal, $V_{ref}(\tau) = S(\tau) \otimes A_s(\tau)$, and a test signal, $V_{test}(\tau) = \{S(\tau) \otimes A_s(\tau)\} \otimes H(\tau) = V_{ref}(t) \otimes H(\tau)$, are deconvolved to yield the desired optical response, $H(t)$, and its Fourier transform, $\tilde{H}(f)$.

The experiment (Fig. 1) follows our earlier work reported in [13,17]. The signal and the LO sources are two mode-locked fiber lasers with repetition rates of $f_S \sim f_L \sim 100$ MHz. We establish a tight optical coherence between these two mode-locked lasers by phase locking a pair of comb teeth from each to two narrow-linewidth cw lasers (at 1550.5 and 1535 nm) such that the relative carrier phase jitter is ~0.4 rad (0.3 fs) and the relative timing jitter is ~20 fs, which is much less than ΔT [17]. The low relative carrier phase jitter is maintained at times longer than 0.1 s through software phase correction, compensating for slow fluctuations in the out-of-loop beam paths. The phase locks have matching rf offsets, but the signal comb has one "extra" comb tooth between the lock points to achieve $M = 19,007$ exactly. From the counted repetition rates and a wave meter reading of the 1551 nm reference laser, the time step is $\Delta T = 525$ fs, $T_{update} = 0.19$ ms and $\nu_0 = 191,458.43$ GHz or 1565 nm (exactly Mf_L below the 1550.5 nm reference laser frequency). To accurately measure the pulses without aliasing issues, we filter to ~2 nm FWHM [~$1/(8\Delta T)$]. The detected LO pulse energy is 350 fJ, and the detected signal pulse energies are 8 and 34 fJ for the reference and test paths, respectively. The data are digitized synchronously with f_L over 512×10^6 samples (set by the digitizer memory) in ~5.1 s, giving a total number of frames of $N_{frames} = 512 \times 10^6/M \sim 26,900$.

Figure 2 compares a single data frame and the fully averaged data frame showing the reference and test signals. The shot-noise-limited SNR (peak signal versus noise) for a single frame in the limit of a strong LO is $2\sqrt{\eta n_S} \sim 448$, where $n_S \sim 63,000$ is the number of signal photons per pulse and $\eta \sim 0.8$ is the detection efficiency; our measured SNR is only ~2× worse than this shot-noise limit (owing to the excess detection noise) and corresponds to a peak sensitivity of ~1.25 photons per time bin. For the averaged signal, the peak height is reduced to ~95%, owing to residual carrier jitter, while the averaged noise drops by the expected factor of $\sqrt{N_{frames}} = 164$, yielding an average SNR on the reference of $36,700 = 2^{15.16}$ and a corresponding peak sensitivity of $[(0.95)^2\eta N_{frames}]^{-1} = 5 \times 10^{-5}$ photons or 6 yJ per time bin. In the frequency domain, the statistical uncertainty of the spectral phase, at the peak, decreases from 65 mrad for a single frame to 0.51 mrad for the averaged
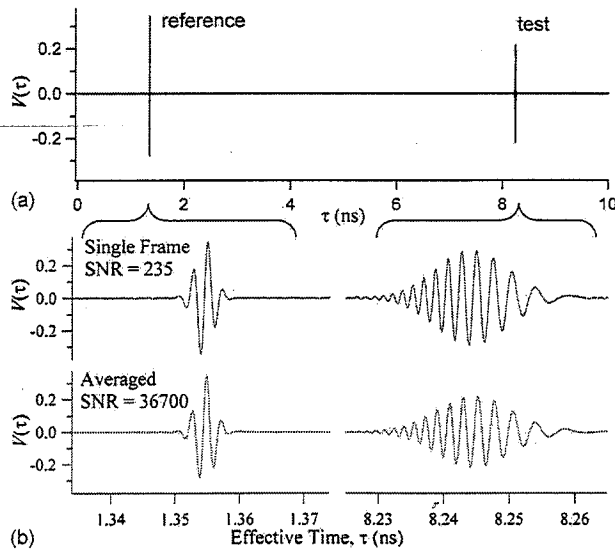
Fig. 2. (Color online) (a) Complete 10 ns, single frame of sampled data at 525 fs spacing. The first peak is from the reference path and the second from the test path. (b) Expanded view of the signal returns for a single frame (upper blue trace) and for an average of 26,900 frames (lower red trace) over 5.1 s after phase correction. The peak retains 95% of its height even after averaging, owing to the high mutual coherence. The test signal return is stretched because of the fiber dispersion. Carrier frequencies seen here are effectively mixed down by ν_0 through the sampling process.

frame with a 3 mrad ripple from etalon effects or slow baseline drift.

Figure 3 shows the optical response function of the fiber spool (and fiber couplers) based on the averaged data of Fig. 2 in both the time and the frequency domains. The statistical uncertainty is 0.70 mrad for the spectral phase and 0.07% for the amplitude across the center. In addition, there is a ~4 mrad ripple at ~100 GHz period, which could be attributed to a differential etalon effect in the test versus reference path; however, more careful work is needed to
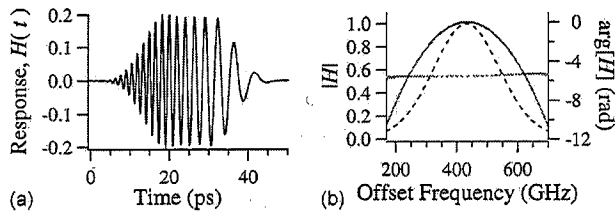

Fig. 3. (Color online) (a) Time domain optical response from deconvolving the averaged data in Fig. 2, after removing the overall phase shift and delay. The peak statistical SNR for the time domain data is 5000. A 50 ps window is shown, but the full available time window is 3 ns, set by the spacing between the reference and test peaks. (b) Frequency domain optical response over 0.5 THz in magnitude (dotted red curve), after removing the relative power splitting of the coupler, and phase (solid blue curve). The 3 ns time window gives a 330 MHz resolution. Also shown is the magnitude spectrum of the of the 2 nm filtered signal (dashed black curve). As in Fig. 2 the carrier and offset frequencies are offset by ν_0.

full establish the systematic uncertainties. The measured dispersion, from a fit to the spectral phase data, is 5.4 ps/(nm km) in agreement with the nominal fiber specifications.

In conclusion, the method of using two mutually coherent frequency combs can provide a high-resolution measurement of linear optical response. This system could have applications for precision measurements in particular when a high frequency resolution or accuracy is needed. The same approach can be applied to measuring nonlinear optical responses or to measuring active signals [19], although with the significant added challenge of establishing coherence between the LO laser and the active source and characterizing the sampling function $S(t)$.

References

1. C. Dorrer, D. C. Kilper, H. R. Stuart, G. Raybon, and M. G. Raymer, IEEE Photon. Technol. Lett. **15**, 1746 (2003).
2. C. Dorrer and I. Kang, J. Opt. Soc. Am. B **25**, A1 (2008).
3. I. Walmsley, L. Waxer, and C. Dorrer, Rev. Sci. Instrum. **72**, 1 (2001).
4. L. Lepetit, G. Cheriaux, and M. Joffre, J. Opt. Soc. Am. B **12**, 2467 (1995).
5. D. Fittinghoff, J. Bowie, J. Sweetser, R. Jennings, M. Krumbugel, K. DeLong, R. Trebino, and I. Walmsley, Opt. Lett. **21**, 884 (1996).
6. T. Udem, R. Holzwarth, and T. W. Hänsch, Nature **416**, 233 (2002).
7. S. A. Diddams, Th. Udem, J. C. Bergquist, E. A. Curtis, R. E. Drullinger, L. Hollberg, W. M. Itano, W. D. Lee, C. W. Oates, K. R. Vogel, and D. J. Wineland, Science **293**, 825 (2001).
8. W. C. Swann, J. J. McFerran, I. Coddington, N. R. Newbury, I. Hartl, M. E. Fermann, P. S. Westbrook, J. W. Nicholson, K. S. Feder, C. Langrock, and M. M. Fejer, Opt. Lett. **31**, 3046 (2006).
9. I. Coddington, W. C. Swann, L. Lorini, J. C. Bergquist, Y. L. Coq, C. W. Oates, Q. Quraishi, K. S. Feder, J. W. Nicholson, P. S. Westbrook, S. A. Diddams, and N. R. Newbury, Nat. Photonics **1**, 283 (2007).
10. S. Schiller, Opt. Lett. **27**, 766 (2002).
11. A. Schliesser, M. Brehm, F. Keilmann, and D. van der Weide, Opt. Express **13**, 9029 (2005).
12. F. Keilmann, C. Gohle, and R. Holzwarth, Opt. Lett. **29**, 1542 (2004).
13. I. Coddington, W. C. Swann, and N. R. Newbury, Phys. Rev. Lett. **100**, 013902 (2008).
14. P. Giaccari, J.-D. Deschenes, P. Saucier, J. Genest, and P. Tremblay, Opt. Express **16**, 4347 (2008).
15. T. Yasui, Y. Kabetani, E. Yokoyoshi, S. Yokoyama, and T. Araki, Appl. Phys. Lett. **88**, 241104 (2006).
16. A. Bartels, R. Cerna, C. Kistner, A. Thoma, F. Hudert, C. Janke, and T. Dekorsy, Rev. Sci. Instrum. **78**, 035107 (2007).
17. I. Coddington, W. C. Swann, L. Nenadovic, and N. R. Newbury, Nat. Photonics **3**, 351 (2009).
18. C. Dorrer, J. Opt. Soc. Am. B **16**, 1160 (1999).
19. P. A. Williams, T. Dennis, I. Coddington, W. C. Swann, and N. R. Newbury, IEEE Photon. Technol. Lett. **20**, 2007 (2008).